Electrostatic modeling of dipole-ion interactions in gramicidinlike channels

M. Sancho and G. Martínez
Departamento de Física Aplicada III, Facultad de Física, Universidad Complutense, 28040, Madrid, Spain

ABSTRACT Using an electrostatic model for the pore and membrane region in a gramicidinlike channel, the effect of dipoles located inside the membrane on the ion transport are analyzed. Calculated energy profiles for different orientations of dipoles show a predominant influence of their radial components. The results qualitatively agree with experimental measurements of conductance on different modified gramicidins and allow to understand the important role of polar side chains on ion permeation.

INTRODUCTION

Gramicidin has been used as a model compound for understanding the motion of ions through cell membranes. However, despite the relative simplicity of its structure and the wealth of experimental data available, many difficulties in the interpretation of results have arisen and basic questions, such as the relative importance of short- and long-range interactions in the ion permeation, remain open (Jordan, 1987).

One method for analyzing the molecular mechanisms by which the peptide interacts with permeating ions involves the substitution of amino acids in certain positions. Recent investigations on linear gramicidins including variants at positions 1, 9, 11, 13, and 15 have shown an important effect of side chain dipole moments on the conductance (for reviews, see Andersen et al., 1987 and Heitz et al., 1988). This poses the question of how groups that project from the exterior surface of the helix and are spatially separate from the axis (5–10 Å) are able to determine the channel's conductance.

Thus, the current understanding of the subject suggests the need for a deeper study of the physical mechanisms underlying the transport and the development of models to quantify dipolar effects to explain the experimental results. Monte Carlo and molecular dynamics simulations, that have been used to analyze electrostatic and dynamic interactions between the ion and the polypeptide, have provided valuable information but failed to give quantitatively, and in some cases qualitatively, correct predictions, probably in part because they have not included the long-range macroscopic interaction with the membrane (Jordan, 1988). The electrostatic models which, despite their oversimplification, have given such good results in related areas (Matthew, 1985), are also valuable in this field. They give regular energy profiles, showing probably the most relevant contributions, predict energy barriers of the adequate order of magnitude to explain the observed conductances, and make it possible to analyze the influence of polar residues in a systematic way.

In this paper we present a macroscopic model for the calculation of the potential profile in an ion channel. It is based on an integral formulation of the electrostatic problem similar to that proposed by Levitt (1978) and improved by Jordan (1982). But our equations are directly expressed in terms of potentials instead of charge densities at the interfaces, thus avoiding the complicated treatment of singularities and allowing the fulfillment of exact boundary conditions. The model includes the effect of dipole contributions which represent approximately the interaction of polar residues with the ion. The study of the influence of different parameters on the results can help in the understanding of the transport mechanisms of ion channels.

METHODS

Model parameters

We have chosen the two-dielectric system represented in Fig. 1 *a* as the initial model for the Gramicidin. The bulk water and the water within the channel are assumed to have the same dielectric constant $\epsilon_1 = 80$; the membrane and the pore former are also described as a uniform medium with a dielectric constant $\epsilon_2 = 2$. In the three-dielectric model (Fig. 1 *b*), a different value has been assigned to the dielectric constant in the pore region, corresponding to the special state of water molecules in the vicinity of the ion and channel walls and immersed in a very strong electric field (Hasted, 1973). The channel half-width has been taken as $h = 12.5$ Å.

The concept of electrostatic radius has been used to account for the fact that the polypeptide backbone has a dielectric constant greater than that of the membrane and so we take r greater than the physical radius of ~ 2 Å (Levitt, 1978). This electrostatic radius could also account for the barrier reduction effect due to a radial polarization of the channel walls produced by the peptide bonds. We will study the effect of varying the value of r on the energy profile. We have also included a net axial polarization associated with each monomer of 3.8

0006-3495/91/07/81/08 $2.00

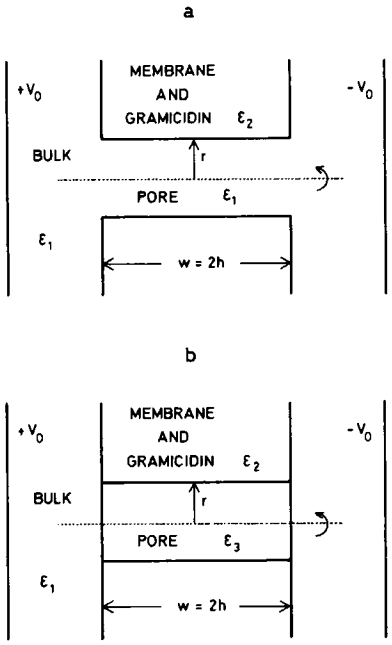

FIGURE 1 Cross-section of the cylindrical system used in the modeling of a GA channel. (*a*) The pore region and the water are represented by the same dielectric constant ϵ_1. (*b*) The channel interior is characterized by a lower dielectric constant ϵ_3.

D (directed to the ethanolamine end), according to the value given by Heitz et al. (1988), due to the charge distribution in the backbone. On the other hand, dipole contributions due to the side chains, in variable positions along the channel length, have been considered.

To retain the rotational symmetry which allows for a relatively simple treatment, side chain dipole moments have been assumed to be uniformly distributed along a ring coaxial with the pore. Similarly, the backbone dipoles are represented as dipolar rings of radius 3.5 Å, each ring located at the midpoint of their respective monomers. It is convenient to note that the cylindrical symmetry of the interface would produce, even for a point source, a polarization with a certain angular distribution, and thus a net interaction dipole-ion not so dependent on the direction, making our approximation of cylindrical symmetry less restrictive than it would seem.

Equations for the electrostatic potential

The electrostatic potential in the channel region is produced by several sources: the ion, the surface charge distribution on the electrodes, the dipoles of the amino acid side chains and those associated with the charge distribution in the backbone, and the polarization of the dielectric media which is equivalent to a charge distribution along the phase boundaries.

The solution to an electrostatic problem of this kind can be approached using a differential formulation or by means of an equivalent set of integral equations. If the geometry includes several charged conductors and dielectric media, the following system of integral equations for the potential can be found (Martínez and Sancho, 1991),

$$\phi(\vec{r}) = \frac{1}{2\pi\epsilon_0(\kappa_i+\kappa_j)}\int_v \frac{\rho(\vec{r}')}{R}dv' + \frac{1}{2\pi\epsilon_0(\kappa_i+\kappa_j)}\int_{S_c}\frac{\sigma(\vec{r}')}{R}ds' - \frac{1}{2\pi(\kappa_i+\kappa_j)}\sum_{S_{lm}}(\kappa_l-\kappa_m)\int_{S_{lm}}\phi(\vec{r}')\frac{\partial}{\partial n'}\left(\frac{1}{R}\right)ds', \quad \vec{r}\in S_{ij} \quad (1)$$

$$\phi(\vec{r}) = \text{const.} = \frac{1}{4\pi\epsilon_0\kappa_i}\int_v\frac{\rho(\vec{r}')}{R}dv' + \frac{1}{4\pi\epsilon_0\kappa_i}\int_{S_c}\frac{\sigma(\vec{r}')}{R}ds' - \frac{1}{4\pi\kappa_i}\sum_{S_{lm}}(\kappa_l-\kappa_m)\int_{S_m}\phi(\vec{r}')\frac{\partial}{\partial n'}\left(\frac{1}{R}\right)ds', \quad (2)$$

$\vec{r}\in S_c$ in contact with the dielectric i,

where $R = |\vec{r}-\vec{r}'|$. S_c represents all the conducting surfaces, S_{ij} is the interface between the media of dielectric constants κ_i and κ_j, and V the total volume. In the last terms, n' is the normal to the interface S_{lm} taken from the medium l toward the medium m.

In Eqs. 1 and 2 the first term of the right-hand side gives the contribution of the space sources (point or volume distributed charges, dipoles, etc); the second, that of the polarized conductors with charge density $\sigma(r')$, and the third the influence of the dielectric interfaces. This formulation incorporates boundary conditions through Eq. 2 with the potential given on the electrodes, and does not enclose singularities as $\phi(\vec{r})$ is a continuous variable.

For the two-dielectric system of Fig. 1 *a*, Eqs. 1 and 2 reduce to

$$\phi(\vec{r}) = \frac{2\kappa}{\kappa+1}\phi_s(\vec{r}) + \frac{1}{2\pi\epsilon_2(\kappa+1)}\int_{S_c}\frac{\sigma(\vec{r}')}{R}ds' + \frac{\kappa-1}{2\pi(\kappa+1)}\int_{S_{12}}\phi(\vec{r}')\frac{\partial}{\partial n'}\left(\frac{1}{R}\right)ds', \quad \vec{r}\in S_{12} \quad (3)$$

$$\phi(\vec{r}) = \text{const.} = \phi_s(\vec{r}) + \frac{1}{4\pi\epsilon_1}\int_{S_c}\frac{\sigma(\vec{r}')}{R}ds' + \frac{\kappa-1}{4\pi\kappa}\int_{S_{12}}\phi(\vec{r}')\frac{\partial}{\partial n'}\left(\frac{1}{R}\right)ds', \quad \vec{r}\in S_c, \quad (4)$$

where $\kappa = \epsilon_1/\epsilon_2$; ϕ_s is the source term, including the potential produced by the ion and the dipoles, in the medium of dielectric constant ϵ_1.

For the three dielectric model of Fig. 1 *b*, a corresponding system can be obtained with an additional coupled integral equation.

Numerical solution

To obtain a solution to the integral Eqs. 3 and 4 or similar equations for the case of three dielectric phases, we have applied a moment method (Harrington, 1968). This technique involves first dividing the dielectric and conducting boundaries into small elements where the potential or the charge density are assumed to be approximately constant. Progressively smaller subareas near the regions where a rapid variation of these quantities are expected (in the vicinity of the edges and sources) have been chosen. Thus the integral system is converted into the following set of algebraic equations

$$\phi_i = \frac{2\kappa}{\kappa+1}\phi_s(\vec{r}_i) + \sum_{j=1}^{k}A_{ij}\phi_j + \sum_{j=k+1}^{n}B_{ij}\sigma_j, \quad i=1,k \quad (5)$$

$$\phi_i = \text{const.} = \phi_s(\vec{r}_i) + \sum_{j=1}^{k}C_{ij}\phi_j + \sum_{j=k+1}^{n}D_{ij}\sigma_j, \quad i=k+1,n, \quad (6)$$

where subelements 1 to k correspond to dielectric interfaces and those from $k+1$ to n refer to conducting ones. In our geometry of Fig. 1 *a*,

the external radius of the membrane surface and the radii of two electrodes set at $\pm 6h$, are taken as $12h$ (a greater length does not modify appreciably the results). The total number of dielectric and conducting subelements used are 82 and 24, respectively. Taking advantage of the configuration symmetry, the number of matrix coefficients to be computed is halved.

The coefficients A_{ij}, B_{ij}, C_{ij}, and D_{ij} are evaluated by means of analytical expressions based on their physical meanings and the matrix system is solved by a Crout reduction technique (for details see Martínez and Sancho, 1991).

Once the system of Eqs. 5 and 6 has been solved, the potential at any space point can be found by means of an equation formally identical to Eq. 6.

Transport equations

Two approaches are currently used for relating experimental fluxes to the structure of the channel: continuum electrodiffusion and reaction rate theory (see Cooper et al., 1985; Levitt, 1986). We prefer the continuum Nernst–Planck equations to obtain conductances corresponding to our barrier shapes. Although the rate constants can be related to the shape of the barriers (Läuger, 1982), the continuum approach may provide a more physical interpretation of the dependence conductance-voltage. Besides, assuming a value of the diffusion coefficient 10 times less than its bulk value, a simple calculation gives an estimation of $\simeq 0.1$ Å for the mean free length of K^+ ions, which makes it more reasonable to view the translocation of the ion as a diffusion rather than a jump between binding positions at a distance of 10 Å apart without intermediate thermal collisions.

The equation which gives the ion flux is (Levitt, 1986)

$$J = DA \frac{C_1 e^{v_1} - C_2 e^{v_2}}{\int e^{v} dz}, \qquad (7)$$

where $v = e\phi/kT$; D is the diffusion coefficient and A the area available for the ion; 1 and 2 represent the extreme positions of the ion trajectory.

RESULTS

The total potential energy viewed at any position by the ion has been obtained as the sum of four separate contributions:

$$U = e(\tfrac{1}{2}\phi_i + \phi_v + \phi_b + \phi_g), \qquad (8)$$

where the first term is affected by the 1/2 factor as it represents the image selfenergy due to the dielectric polarization produced by the ion. ϕ_v is the potential produced by the applied voltage; ϕ_b and ϕ_g are the contributions of the dipole moments associated with the backbone and side groups, respectively. The computation of all these contributions is performed separately, using Eqs. 5 and 6 for each of them. In these equations ϕ_s is the corresponding source term and the electrodes are placed at 0 V, except in calculating ϕ_v for which ϕ_s is null and the electrodes are at $\pm V_0$.

Image profiles obtained for different radii of the channel in the two-dielectric model, are shown in Fig. 2. They represent the main constraint to the ion passage along the channel with barriers of $\simeq 6.5$–9 kT. The continuous curve essentially coincides with results previously published by Jordan et al. (1989) for the case of zero ionic strength. The barrier height shows an important reduction as the pore radius increases. In subsequent studies, we have used an electrical radius $r =$ 2.8 Å. This represents a limit situation in which the additional dipole contributions modulate the conductance in a similar way to that experimentally obtained, as will be seen below.

In Fig. 3, predictions of two- and three-dielectric models for the image selfenergy, are compared. For the studied case, the lower dielectric constant within the pore, $\epsilon_3 = 40$, produces a barrier height $\simeq 1.5$ times greater than for $\epsilon_3 = \epsilon_1 = 80$. The profile is also constrained inside the pore length, showing a singularity at $z = h$, due to the approximation of point charge. In a more realistic modeling with a finite ion size there would be a finite barrier corresponding to the difference in Born charging energies at both sides, with a well slightly inside the channel producing a binding position for an ion near the pore mouth.

The high barriers obtained with a lowered dielectric constant for the water inside the pore do not invalidate this model. It should be kept in mind that the electrical radius accounts for the effect of the dielectric constant of the polypeptide, making this equivalent to a layer of the medium which fills the pore. It is clear that in the case $\epsilon_3 = 40$, the electrical radius should be greater, thus lowering the barrier. We have found that a barrier height of the same order as in the two-dielectric case is obtained with $r \simeq 3.5$ Å. In addition, the electrostatic

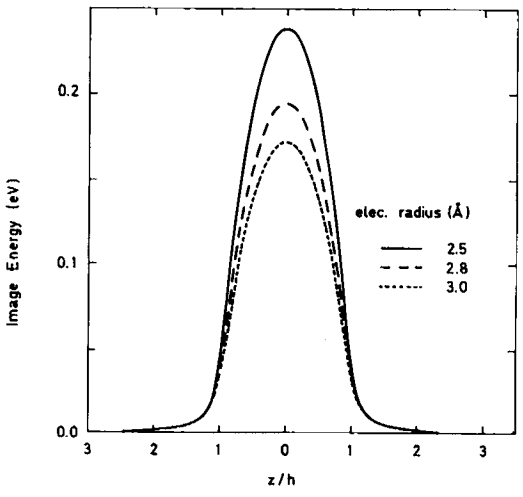

FIGURE 2 Image energy profile as a function of the electrical radius in the two-dielectric model.

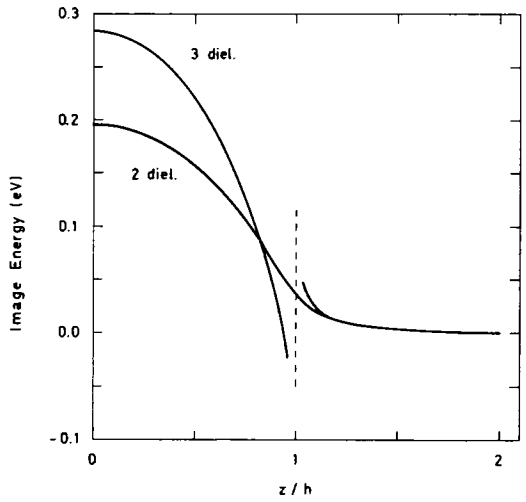

FIGURE 3 Image energy profiles obtained for the two- and three-dielectric models with an electrical radius of 2.8 Å.

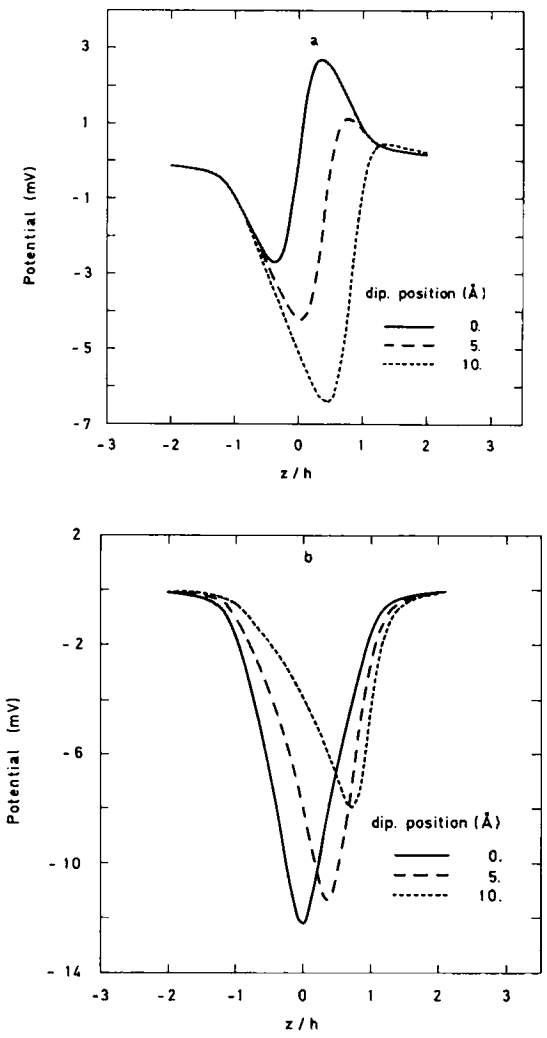

FIGURE 4 Potential created by a dipole ring with a radius of 5 Å and situated at different positions along the channel. (*a*) $p_z = +1\text{D}, p_r = 0$. (*b*) $p_z = 0, p_r = +1\text{D}$.

actions on the ion will be in that case less screened, giving stronger dipole influences. Thus, similar overall conclusions with respect to the qualitative analysis of dipole effects can be deduced using either of the models, with appropriate values of the parameters. For the sake of simplicity, we will restrict ourselves in the following to the use of the two phases scheme.

We have studied the contribution ϕ_g to the potential profile produced by a single axial dipole ring with moment +1D (positive moment means that the positive end of the dipole is pointing toward the nearest end of the channel), in different positions along the channel (Fig. 4 *a*). When the dipole position shifts to the external side of the channel, the curve loses its initial symmetry and surprisingly the negative values of the potential increase. This effect is due to the influence of the polarization charges induced on the lateral interface membrane bulk and are less pronounced for a longer channel.

For a radial component with moment +1D (positive end of the dipole pointing away from the axis), the variation is the opposite as shown in Fig. 4 *b*: when the dipole is near the mouth, the minimum of the potential curve is higher. We note that for the wide range of positions represented in Figs. 4, *a* and *b*, a radial component of dipole moment is more effective in reducing (or increasing, for opposite dipole direction) the barrier than the same value of a *z* component.

Also, we have studied the influence of the distance of the dipoles from the channel axis. Figs. 5, *a* and *b*, show the variation of the potential curves with the dipole ring radius, for a ring at an axial position of 5 Å.

Figs. 6, *a* and *b*, depict the contribution ϕ_g for a symmetric channel with dipole rings p_z and p_r associated with each monomer, respectively. It is interesting to observe that in a position near the center of the channel, the superposed effects of both dipole *z* components which point in opposite directions nearly cancel each other, whereas the corresponding *r* components produce a pronounced minimum. It is also noticeable that the effect of p_z dipoles situated near the channel mouth is highest just in the middle, with a rather wide profile. The curves for p_r show two potential minima corresponding to the dipole positions, except for dipoles close to the channel center.

The analysis of the Nernst–Planck equation using Gaussian potential profiles of variable height and width

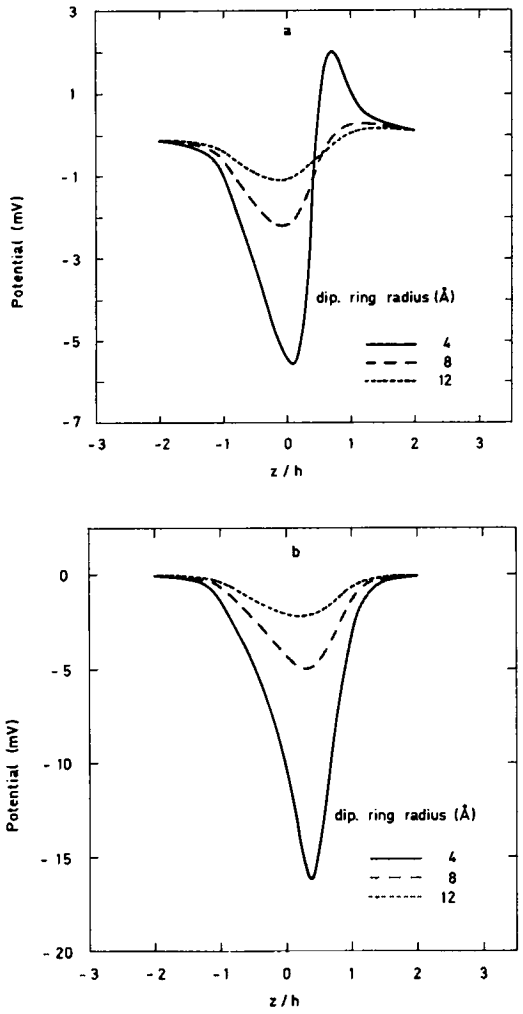

FIGURE 5 Variation of the profiles ϕ_g with the radius of the dipole ring. The source is located at $z = 5$ Å. (*a*) $p_z = +1\text{D}, p_r = 0$. (*b*) $p_z = 0$, $p_r = +1\text{D}$.

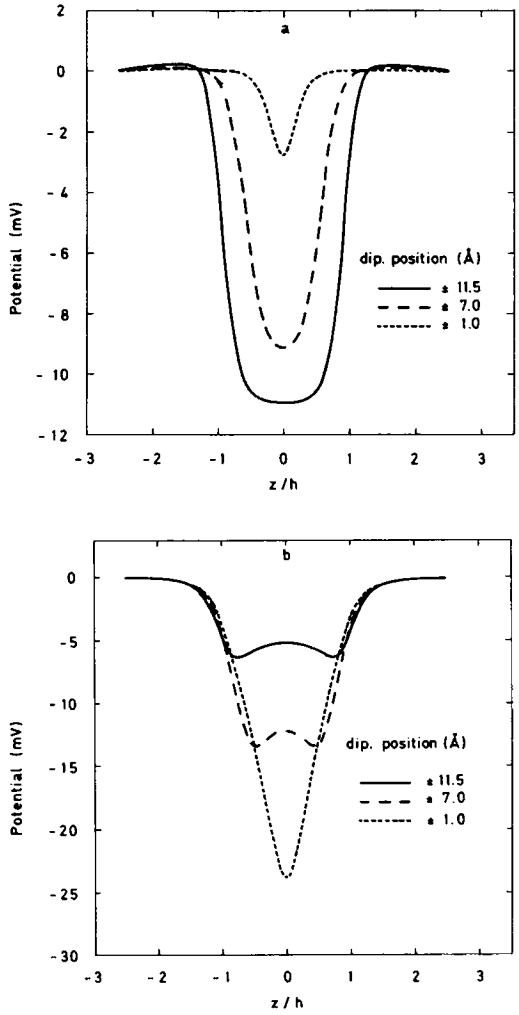

FIGURE 6 Potential created by two dipole rings with radii of 5 Å and different positions $\pm z$ along the channel. (*a*) $p_z = +1\text{D}, p_r = 0$. (*b*) $p_z = 0, p_r = +1\text{D}$.

as test energy functions, shows that a linear I-V characteristic is obtained when the barrier is low and/or sufficiently narrow. In our case, total energy profiles obtained from Eq. 8 show variable height and width depending on applied potentials and dipole magnitudes and/or orientations. A systematic study has been done, applying Eq. 7 to these profiles. The integration along z has been carried out by a standard routine between electrode positions 1 and 2, situated at $\pm 6h$, respectively. The analysis of the results gives the following general features:

(*a*) High currents are associated with linear or even sublinear behavior (conductance decreases at high voltages) and low currents with an increase of the conductance with the applied voltage.

(*b*) High positive dipole moments, in each of the components r or z, give high currents and linear behavior. If the moment is lowered, the current decreases and below a certain value the I-V characteristic becomes nonlinear. In general, for a given value of moment, a radial orientation produces a higher current than an axial one, except for positions near the mouth where the axial contribution dominates.

(*c*) Axial dipole components in positions $\simeq \pm 1$ Å near the channel midpoint are nearly ineffective whereas radial components have an important role in giving high current and linear characteristics. This could also be deduced from the analysis of Figs. 6, *a* and *b*.

(*d*) For more external positions ($\simeq \pm 7$ to ± 11.5 Å), shifting positive radial components toward the center of the channel produces an increase in conductance, whereas for z components the variation is the opposite.

This could also be expected from the variation of the energy profiles in Figs. 4, *a* and *b*.

Fig. 7 and Table 1 summarize these characteristics. In Fig. 7 *a* calculated conductances for different values and orientations of dipole moments are shown. The dipole rings are in all cases situated in representative mean positions of ±8.5 Å. They give approximately the same potential as 10 rings distributed along the channel length simulating the presence of polar residues (Triptophanes and Valines). In Fig. 7 *b* normalized values of conductance are given for different cases. The effect of the position of dipole rings of 2.1 D (which represents the dipole moment of a Trp residue) on the conductance is illustrated in Table 1.

TABLE 1 Channel conductance as a function of the dipole ring positions, for axial and radial orientations

Dipole positions	Conductance	
	$p_z = 2.1\ D$	$p_r = 2.1\ D$
±11.5	9.3	6.2
±10.0	8.5	7.6
± 8.5	7.7	9.1
± 7.0	7.0	10.7
± 1.0	4.4	14.6

The values are given in the same arbitrary units as in Fig. 7 *a*.

To explain the reason for the different conductances, net profiles corresponding to several dipole moments and a polarization of 50 mV, have been depicted in Fig. 8. The barrier heights for the cases p = 8.5 D, θ = 90° and p = 6.0 D, θ = 45° are similar; however, the second has a wider profile giving in consequence a lower conductance, as was obtained in Fig. 7.

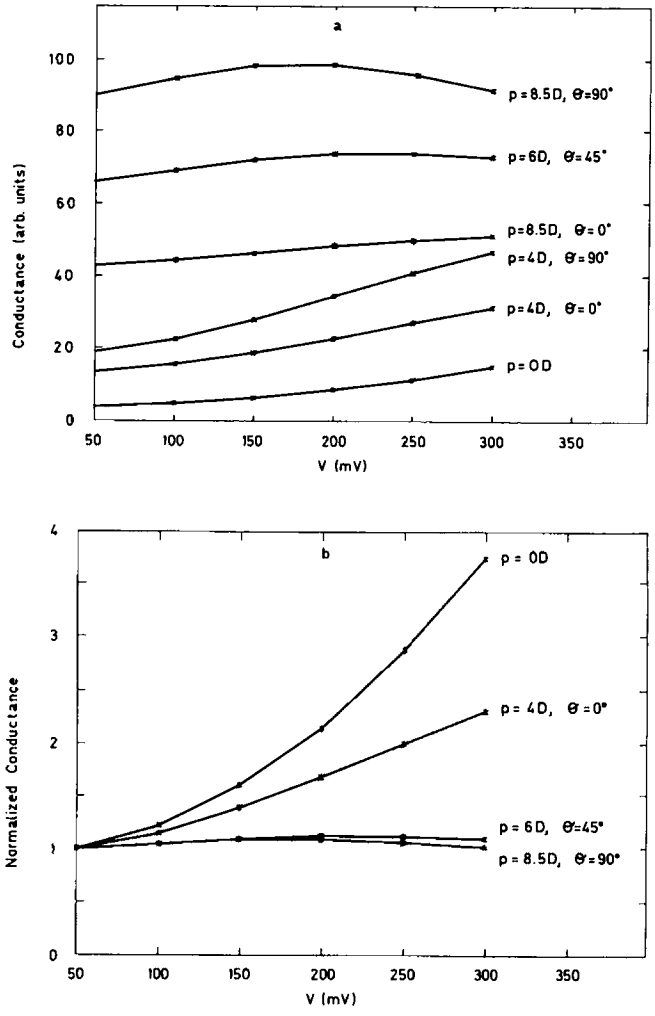

FIGURE 7 (*a*) Conductance vs. the applied voltage for different values of the dipole moment and orientation. (*b*) Idem normalized to its value at 50 mV. The dipolar sources are situated at ±8.5 Å and have a radius of 5 Å. θ is the angle between the dipole moment and the *z*-axis in the right-hand side of the channel. The orientation of the left-hand side moment is given by the reflection of this source with respect to the plane $z = 0$.

DISCUSSION

In Gramicidin A the residues 9, 11, 13, 15 have a polar aromatic side group, indol, the remaining residues having unpolar (or nearly) side groups. Because the first work on Gramicidin variants by Bamberg et al. (1976), diverse natural and synthetic analogues with one or several residues replaced by others of different polarity have been studied, trying to clarify the action of polar

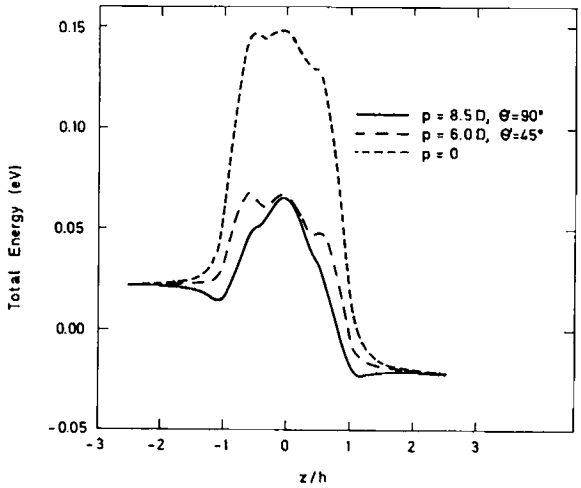

FIGURE 8 Total energy profiles used in the computation of the conductance at 50 mV for some of the curves represented in Fig. 7.

side chains on the permeation (Veatch and Stryer, 1977; Morrow et al., 1979; Heitz et al., 1982; Mazet et al., 1984; Barret et al., 1986; Daumas et al., 1989; Becker et al., 1989; Fonseca et al., 1989). For the sake of comparison with our numerical results, we shall summarize some of the most important conclusions of these experimental studies: (*a*) the bulkiness of the side chains does not appreciably affect the conductance. The important effects on the ion transport seem to be almost entirely due to dipole-ion interactions. (*b*) There are two basic types of behaviors: one of them, corresponding to GA and analogues with high dipole moment, shows a high conductance, approximately constant with the applied voltage; the second one gives a much lower voltage-dependent conductance which implies a nonlinear intensity-voltage characteristic. The transition from one type to the other is observed when at least three Trps are replaced by other groups with lower or null dipole moment. (*c*) A side chain with high dipole moment value is not always associated with high current, especially when the substitution is made at position 1. (*d*) The side chains in each of the mentioned positions contribute differently to the conductance, leading to a lower conductance when a substitution Trp(2.1D) by Phe(0D) is made nearer the channel center.

According to the predictions of our model, dipole moments of the order of magnitude of those assigned to side chains in GA and analogues molecules, can account for the important modification of ion permeation experimentally observed and explain the general characteristics *a* to *d*. To have energy barriers of appropriate magnitude, a dipole component associated with the backbone is necessary. In addition, this component together with Trp dipole moments are responsible in our model for the valence selectivity of Gramicidin. Calculations in a channel without any dipole moment except that of the backbone give a barrier height of 9.3 kT for a single charged anion and a conductance of 0.2 at 50 mV in the arbitrary units of Fig. 7 *a*, making the channel ineffective in transporting negatively charged ions. This interpretation differs from that of Sung and Jordan (1987). In their study, based upon a conformation of Koeppe and Kimura (1984), the backbone dipolar moment used was −1.7D. They obtained an energy profile with a minimum for cations and, therefore, a maximum for anions at the channel entry. Rejection of anions was a consequence of this large barrier at the mouth. In our model, the positive moment assigned to the backbone reduces the central barrier for cations and increases it for anions; however, the energy profile at the mouths is not appreciably modified, in spite of the quadrupolar nature of the configuration (c.f. Fig. 6 *a*). This is due to the overall dielectric polarization effect.

At intermediate positions along the channel, the most favorable orientation of a dipole for high current and ohmic behavior is ~45°. Quasi-linear I-V characteristics can be obtained with different dipole moment values and different orientations (see Figs. 7, *a* and *b*). The experimental I-V curves for Cs^+ transport in GT, $GN^{9,15}$, and $GN^{11,13}$ that show linear behavior with different levels of conductance (Heitz et al., 1988: Fig. 2) are compatible with our interpretation if a reorientation of the remaining dipoles accompanies the substitution of the residues. It is evident that not only the value of dipole moment but also its orientation is important. Residues with high moment may produce similar or even lower conductances than some less polar ones. This is particularly important for substitutions in position 1 where dipole *z* components have very little effect.

The dependence on the position mentioned in *d* suggests a predominance of radial component of Trp dipoles in GA. Thus, from Table 1 we can deduce that if a radial dipole is taken away from positions nearer the center, a lower conductance will be obtained in agreement with the experimental observation. This is also in concordance with the fact that *r* components give higher conductance than *z* components as seen in Fig. 7 *a*. Then the highest conductance of GA among practically all the analogues would be due to the lowering of the energy barrier produced by the dipole moment of Trp residues pointing in a predominantly radial direction. This conflicts with theoretical calculations of in vacuum molecular structure of GA (Etchebest and Pullman, 1985) which predict angles of ~45° for Trp 15 and 9 dipoles which attract the ion and nearly axial orientations which repel it for Trp 11 and 13. However, this configuration has been questioned on the basis of both experimental and theorectical results and the fact that the interaction of the molecule with the lipid membrane and water can substantially influence the equilibrium conformation (Heitz et al., 1988; Daumas et al., 1989). In our model the electrostatic interaction polypeptide membrane has been treated through the effect of dielectrics and interface polarization. This is one of the most important conclusions of our work: the screening of some interactions produced by the different dielectric regions can affect the energy distribution as well as modulate the electrostatic forces due to polar side chains on the ion in a way which differs from that expected in a continuous medium.

Summarizing, we have shown that a macroscopic model can explain some aspects of the observed behavior in GA and analogues. One may wonder how sensitive are the results to the choice of model parameters. The combination chosen for the pore and membrane permittivities, electric radius, dipolar moments of the side

chains and backbone, and ring radii, has been one among various possibilities. All these parameters have interrelated effects. Thus, an increase of the electric radius reduces the image energy but, at the same time, diminishes the contribution of the dipolar rings due to the increased screening of their effect on the channel axis. However, the range of these variations cannot be extended too much if it is desired to keep values of parameters compatible with the accepted structure of the channel. Thus, the model is certainly sensitive to the election of the parameters. This is not unexpected because, in fact, Gramicidin is a system with great sensitivity to different experimental conditions. It seems desirable to test further the simulation by applying the model to other measurements, such as those recently made on hybrid channels. Work is being done in this direction.

We acknowledge the valuable information on experimental results given by V. Fonseca and O. Andersen. We are also grateful to F. Heitz and P. Jordan for their helpful comments.

Received for publication 8 November 1990 and in final form 18 February 1991.

REFERENCES

Andersen, O. S., R. E. Koeppe II, J. T. Durkin, and J. L. Mazet. 1987. Structure-function studies on linear Gramicidins: site-specific modifications in a membrane channel. *In* Ion Transport Through Membranes. Academic Press, New York. 295–314.

Bamberg, E., K. Noda, E. Gross, and P. Läuger. 1976. Single-channel parameters of Gramicidin A, B and C. *Biochim. Biophys. Acta.* 419:223–228.

Barrett Russell, E. W., L. B. Weiss, F. I. Navetta, R. E. Koeppe II, and O. S. Andersen. 1986. Single-channel studies on linear Gramicidins with altered amino acid side chains. *Biophys. J.* 49:673–686.

Becker, M. D., D. B. Sawyer, A. K. Maddock, R. E. Koeppe II, and O. S. Andersen. 1989. Single Tryptophan-to-Phenylalanine substitutions in Gramicidin channels. *Biophys. J.* 55:503*a*. (Abstr.)

Cooper, K., E. Jakobsson, and P. Wolynes. 1985. The theory of ion transport through membrane channels. *Prog. Biophys. Molec. Biol.* 46:51–96.

Daumas, P., F. Heitz, L. Ranjalahy-Rasoloarijao, and R. Lazaro. 1989. Gramicidin A analogs: influence of the substitution of the tryptophans by naphtylalanines. *Biochimie.* 71:77–81.

Etchebest, C., and A. Pullman. 1985. The effect of the amino acid side chains on the energy profiles for ion transport in the Gramicidin A channel. *J. Biomol. Struct. Dyn.* 2:859–869.

Fonseca, V., P. Daumas, L. Ranjalahy-Rasoloarijao, F. Heitz, R. Lazaro, Y. Trudelle, and O. Andersen. 1989. Gramicidin channels that have no Tryptophan residues. *Biophys. J.* 55:502*a*. (Abstr.)

Harrington, R. F. 1968. Field computation by moment methods. Macmillan, New York. 229 pp.

Hasted, J. B. 1973. Aqueous dielectrics. Chapman and Hall, London. 15–16.

Heitz, F., G. Spach, and Y. Trudelle. 1982. Single channels of 9, 11, 13, 15-Destryptophyl-Phenilalanyl-Gramicidin A. *Biophys. J.* 40:87–89.

Heitz, F., P. Daumas, N. Van Mau, R. Lazaro, Y. Trudelle, C. Etchebest, and A. Pullman. 1988. Linear gramicidins: influence of the nature of the aromatic side chains on the channel conductance. *In* Transport through membranes: carriers, channels and pumps. A. Pullman, J. Jortner, and B. Pullman, editors. Kluwer Academic Publishers Group, Dordrecht, the Netherlands. 147–165.

Jordan, P. C. 1982. Electrostatic modeling of ion pores. Energy barriers and electric field profiles. *Biophys. J.* 39:157–164.

Jordan, P. C. 1987. Microscopic approaches to ion transport through transmembrane channels. The model system Gramicidin. *J. Phys. Chem.* 91:6582–6591.

Jordan, P. C. 1988. A molecular dynamics study of Cesium ion motion in a Gramicidin-like channel. Structural and energetic implications. *In* Transport through membranes: channels, carriers and pumps. A. Pullman, J. Jortner, and B. Pullman, editors. Kluwer Academic Publishers Group, Dordrecht, the Netherlands. 237–251.

Jordan, P. C., R. J. Bacquet, J. A. McCammon, and P. Tran. 1989. How electrolyte shielding influences the electrical potential in transmembrane ion channels. *Biophys. J.* 55:1041–1052.

Koeppe, R. E. II, and M. Kimura. 1984. Computer building of β-helical polypeptide models. *Biopolymers.* 23:23–38.

Läuger, P. 1982. Microscopic calculation of ion-transport rates in membrane channels. *Biophys. Chem.* 15:89–100.

Levitt, D. G. 1978. Electrostatic calculations for an ion channel. I. Energy and potential profiles and interactions between ions. *Biophys. J.* 22:209–219.

Levitt, D. G. 1986. Interpretation of biological ion channel flux data. Reaction-rate versus continuum theory. *Annu. Rev. Biophys. Biophys. Chem.* 15:29–57.

Martínez, G., and M. Sancho. 1991. Application of the integral equation method to the analysis of electrostatic potentials and electron trajectories. *In* Advances in Electronics and Electron Physics. P. Hawkes, editor. Academic Press, New York. 81:1–41.

Matthew, J. B. 1985. Electrostatic effects in proteins. *Annu. Rev. Biophys. Chem.* 14:387–417.

Mazet, J. L., O. S. Andersen, and R. E. Koeppe II. 1984. Single-channel studies on linear Gramicidins with altered amino acid sequences: a comparison of Phenylalanine, Tryptophane and Tyrosine substitutions at position 1 and 11. *Biophys. J.* 45:263–276.

Morrow, J. S., W. R. Veatch, and L. Stryer. 1979. Transmembrane channel activity of Gramicidin A analogs: effects of modification and delation of the amino-terminal residue. *J. Mol. Biol.* 132:733–738.

Sung, S., and P. C. Jordan. 1987. Why is Gramicidin valence selective? A theoretical study. *Biophys. J.* 51:661–672.

Veatch, W., and L. Stryer. 1977. The dimeric nature of the Gramicidin A transmembrane channel: conductance and fluorescence energy transfer studies of hybrid channels. *J. Mol. Biol.* 113:89–102.